Neurotoxicology 74 (2019) 242–251

Contents lists available at ScienceDirect

Neurotoxicology

journal homepage: www.elsevier.com/locate/neuro

Full Length Article

Peroxiredoxin 5 prevents diethylhexyl phthalate-induced neuronal cell death by inhibiting mitochondrial fission in mouse hippocampal HT-22 cells

Dong Gil Lee[a,1], Kyung-Min Kim[a,1], Hyun-Shik Lee[a], Yong Chul Bae[b], Jae-Won Huh[c], Sang-Rae Lee[c], Dong-Seok Lee[a,*]

[a] School of Life Sciences, BK21 Plus KNU Creative BioResearch Group, Kyungpook National University, Daegu, Republic of Korea
[b] Department of Anatomy and Neurobiology, School of Dentistry, Kyungpook National University, Daegu, Republic of Korea
[c] National Primate Research Center, Korea Research Institute of Bioscience and Biotechnology (KRIBB), Chungcheonbuk-do, Republic of Korea

ARTICLE INFO

Keywords:
Peroxiredoxin 5
Diethylhexyl phthalate
Mitochondrial dynamics
Oxidative stress
Neurotoxicity

ABSTRACT

Diethylhexyl phthalate (DEHP) is used in many plastic products, such as perfumes, lunch boxes, bags, and building materials. As DEHP is not covalently bound to the plastic, humans can be easily exposed to it. DEHP induces neurobehavioral changes and neuronal cell death; however, the exact mechanism behind this is still unclear. We hypothesized that the neurotoxic mechanism is related to DEHP-induced oxidative stress leading to apoptosis through mitochondrial fission. We demonstrated that DEHP-induced oxidative stress triggers neuronal cell death via mitochondrial fission in mouse hippocampal HT-22 cells. Furthermore, we identified that peroxiredoxin 5 (Prx5), an antioxidant enzyme induced by DEHP, prevents DEHP-induced mitochondrial fission by inhibiting the production of reactive oxygen species. We conclude that Prx5 may be a promising therapeutic target for mitigating DEHP-induced neuronal cell death.

1. Introduction

Phthalates are environmental esters used as plasticizers. They are routinely used in the production of perfumes, carpets, and shower curtains, among other products. Phthalates are not chemically bound to plastic products, thus facilitating human exposure to these compounds (Lee et al., 2014). Diethylhexyl phthalate (DEHP) is among the phthalates most commonly used as plasticizers (Zhang et al., 2018). Several studies have identified DEHP's reproductive, developmental, and endocrine toxicity (Chen et al., 2015; Erkekoglu et al., 2011; Tyl et al., 1988). Furthermore, DEHP causes neurotoxicity, including harmful effects on hippocampal network plasticity and neurodevelopment (Holahan and Smith, 2015; Rowdhwal and Chen, 2018). However, the precise mechanism of DEHP-mediated neurotoxicity is still unclear.

Mitochondria play important roles in adenosine triphosphate (ATP) production, lipid metabolism, redox homeostasis, and apoptosis (Otera and Mihara, 2012; Picard et al., 2013). They change their morphology in response to conditions, such as stress and proliferation, by either fission or fusion (McCarron et al., 2013). In mammals, dynamin-related protein 1 (Drp1) and mitochondrial fission 1 (Fis1) are involved in fission, whereas mitofusin 1 (Mfn1) and mitofusin 2 (Mfn2) are involved in mitochondrial outer membrane fusion (Westermann, 2008). Drp1 induces cytochrome C release by promoting Bax/Bak during apoptosis (Cho et al., 2010). Also, deleting Mfn1 and Mfn2 increases mitochondrial fission, thus inducing apoptosis (Suen et al., 2008). Imbalances in mitochondrial dynamics are associated with cell death and neuronal synaptic loss in neurodegenerative diseases (Cho et al., 2010; Knott et al., 2008). DEHP induces apoptosis via mitochondrial pathways in GC-2spd cells (Fu et al., 2017). However, the mechanisms underlying the association between changes in DEHP-induced mitochondrial dynamics and neuronal cell death have not been studied yet.

Free radicals created from natural byproducts, abnormal reactions, and environmental stress are highly reactive molecules containing oxygen. Reactive oxygen species (ROS), a subset of free radicals, include peroxyl radicals (ROH), superoxide ($O_2^{\bullet -}$), non-radical molecules, hydrogen peroxide (H_2O_2), and hydroxyl radicals ($^{\bullet}OH$). At low concentrations, they are involved in cell signaling cascades and immune responses; however, at high concentrations, ROS can lead to oxidative stress, resulting in damage to lipids, DNA, and proteins (Berlett and Stadtman, 1997; Coluzzi et al., 2014; Hauck and Bernlohr, 2016). Oxidative stress can also cause mitochondrial dysfunction and caspase activation, thus inducing apoptosis (Ryter et al., 2007). DEHP produces ROS, leading to oxidative stress (Cho et al., 2015). Peroxiredoxins

* Corresponding author.
E-mail address: lee1@knu.ac.kr (D.-S. Lee).
[1] These authors contributed equally to this work.

https://doi.org/10.1016/j.neuro.2019.08.003
Received 18 March 2019; Received in revised form 29 July 2019; Accepted 5 August 2019
Available online 10 August 2019
0161-813X/

(Prxs), a family of antioxidant enzymes, can eliminate H_2O_2 and participate in cellular signaling through intracellular oxidative signaling pathways (Kang et al., 2005; Knoops et al., 2011; Rhee et al., 2005). While Prx overexpression protects various cells, including neuronal cells, knockdown of Prxs generally makes cells more sensitive to cell death by means of oxidative stress (Hampton and O'Connor, 2016; Park et al., 2015). Prxs play important roles in redox-sensitive signaling. However, there has been limited research on the relationship between Prxs and DEHP-induced oxidative stress.

In this study, we investigated, for the first time, the mechanism underlying DEHP-induced oxidative stress and mitochondrial fission with regard to neuronal cell death in hippocampal HT-22 cells. Furthermore, we examined the effect of Prx5 on DEHP-induced neurotoxicity related to oxidative stress-dependent mitochondrial fission.

2. Materials and methods

2.1. Materials

N-Acetyl-L-cysteine (NAC), dimethyl sulfoxide (DMSO), and di-(2-ethylhexyl) phthalate (DEHP) were obtained from Sigma-Aldrich (St. Louis, MO, USA).

2.2. Cell culture and treatment

HT-22 cells were derived from HT-4 cells immortalized from primary mouse hippocampal neuronal cultures (Davis and Maher, 1994). Cells were maintained in Dulbecco's modified Eagle's medium (Welgene, Daegu, Korea) supplemented with 10% fetal bovine serum (Thermo Fisher Scientific Inc., MA, USA) and 1% penicillin/streptomycin (Welgene) at 37 °C in a humidified 5% CO_2 incubator (Panasonic Corporation, Osaka, Japan). The cells were grown to a density of 1×10^4 in a 6-well plate (SPL Life Sciences Co. Pocheon-si, Korea) for 24 h at 37 °C before initiating the experiments.

2.3. Plasmid construction

DsRed2-Mito gene was obtained from pDsRed2-Mito (Clontech, CA, USA). *DsRed2-Mito* and mouse *Prx5* were amplified by polymerase chain reaction (PCR) using LA Taq polymerase (TaKaRa, Shiga, Japan). These genes were cloned into pCR8/GW/TOPO (Thermo Fisher) and inserted into pLenti6.3/V5-DEST (Thermo Fisher) using LR clonase (Thermo Fisher). The constructed vectors were confirmed by restriction mapping and DNA sequencing.

2.4. Transfection and selection of stably expressing cells

HT-22 cells (1×10^5 cells) were seeded in 6-well plates. After 24 h, cells were transfected with 1 μg of plasmids, such as pLenti6.3-*DsRed2-Mito* and pLenti6.3-*Prx5* using Effectene reagent (Qiagen, CA, USA), according to the manufacturer's instructions. After transfection for 1 day, *DsRed2-Mito*- and *Prx5*-transfected HT-22 cells were selected with 8 μg/mL blasticidin (Thermo Fisher).

2.5. Western blotting

Protein lysates were prepared using ice-cold PRO-PREP protein extraction solution (iNtRON Biotechnology Inc, Seongnam, Korea). Protein quantification was performed using an Infinite F50 microplate reader (TECAN, Männedorf, Switzerland). Protein lysates totaling 15–20 μg were separated on 8%–12% sodium dodecyl sulfate (SDS)-polyacrylamide gel. The separated proteins were then transferred onto nitrocellulose membranes (Pall Corporation, NY, USA). Membranes were blocked with 5% skimmed milk (BD Biosciences, New Jersey, USA) and incubated overnight with primary antibodies against Mfn1, Mfn2, and Drp1 (Santa Cruz Biotechnology, Texas, USA); PARP, cleaved caspase 3, Drp1 Ser616, and Drp1 Ser637 (Cell Signaling, MA, USA); β-actin, Prx1, Prx2, Prx3, Prx4, and prx5 (Ab Frontier, Seoul, Korea); and V5 epitope (Thermo Fisher Scientific) at 4 °C. Membranes were washed six times with 10 mM Tris–HCl (pH 7.5) containing 150 mM NaCl and 0.1% Tween-20 (TBST) and subsequently incubated with horseradish peroxidase-conjugated goat anti-rabbit and anti-mouse antibodies (Thermo Fisher Scientific) before being incubated overnight at 4 °C. After removing excess secondary antibodies, membranes were washed six times with TBST. Specific binding was detected using Clarity Western ECL Substrate (Bio-Rad, CA, USA), according to the manufacturer's instructions.

2.6. Flow cytometry

HT-22 cells were treated with or without 100 μM DEHP for 24 h. To measure intracellular ROS levels and mitochondrial ROS levels, we washed harvested cells with phosphate-buffered saline (PBS) and then incubated them with 2.5 μM CM-H2DCFDA and 2.5 μM MitoSOX (Thermo Fisher Scientific) for 15 min at 37 °C. Cells were then washed twice with PBS before being analyzed by flow cytometry (FACSCalibur, FACSVerse; BD Biosciences).

2.7. Cell viability assay

Cell viability was assessed using the D-Plus™ CCK cell viability assay kit (Donginbio, Korea). Mock vector- and Prx5-expressing HT-22 cells (at a density of 5×10^4 cells for each cell type) were cultured in 6-well plates and incubated for 24 h before treatment. Cells were then treated with 100 μM DEHP and incubated for 24 h. Subsequently, cells were treated with 50 μl CCK per well and incubated for 1 h at 37 °C. Absorbance was measured at 450 nm using an Infinite F50 microplate reader (TECAN).

2.8. Imaging and measurement of mitochondrial length

HT-22 cells were seeded on 0.1% poly-D-lysine-coated round coverslips (diameter, 24 mm; Marienfeld, Lauda-Königshofen, Germany) and incubated for 24 h. The cells were then incubated with 100 μM DEHP for 24 h, washed twice with PBS, and fixed with 4% paraformaldehyde in PBS for 1 h. After washing twice with PBS, the coverslips were mounted on slides using VECTASHIELD mounting medium (VECTOR Laboratories, CA, USA). Images were obtained using an LSM-710 confocal microscope (Carl Zeiss, Oberkochen, Germany) equipped with a plan apochromatic 100×/1.40 oil DIC M27 objective lens. Images were processed using a Zeiss LSM image examiner, ZEN 2009 Light Edition (Carl Zeiss). The mitochondrial length was measured using ImageJ software (NIH, MD, USA) and was calculated using more than 50 mitochondrial particles per cells in over 20 cells. The over 20 cells in all experimental group were analyzed as one independent experiment, respectively.

2.9. RNA interference assay

HT-22 cells were grown to 50% confluence and then transfected with 10 pmol of siRNA against Prx5 (siPrx5; Bioneer, Daejeon, Korea) using Lipofectamine RNAiMAX (Thermo Fisher Scientific), according to the manufacturer's instructions. The siRNA sequence is as follows: siPrx5 sense, 5′-GUCUGAGCGUUAAUGACGU-3′ and siPrx5 antisense, 5′-ACGUCAUUAACGCUCAGAC-3′.

2.10. Statistics

Data are represented as the mean ± standard error of the mean (SEM) of at least three independent experiments. Statistically significant differences were determined using one-way or two-way ANOVA in GraphPad Prism 5 software (San Diego, CA, USA).). We used

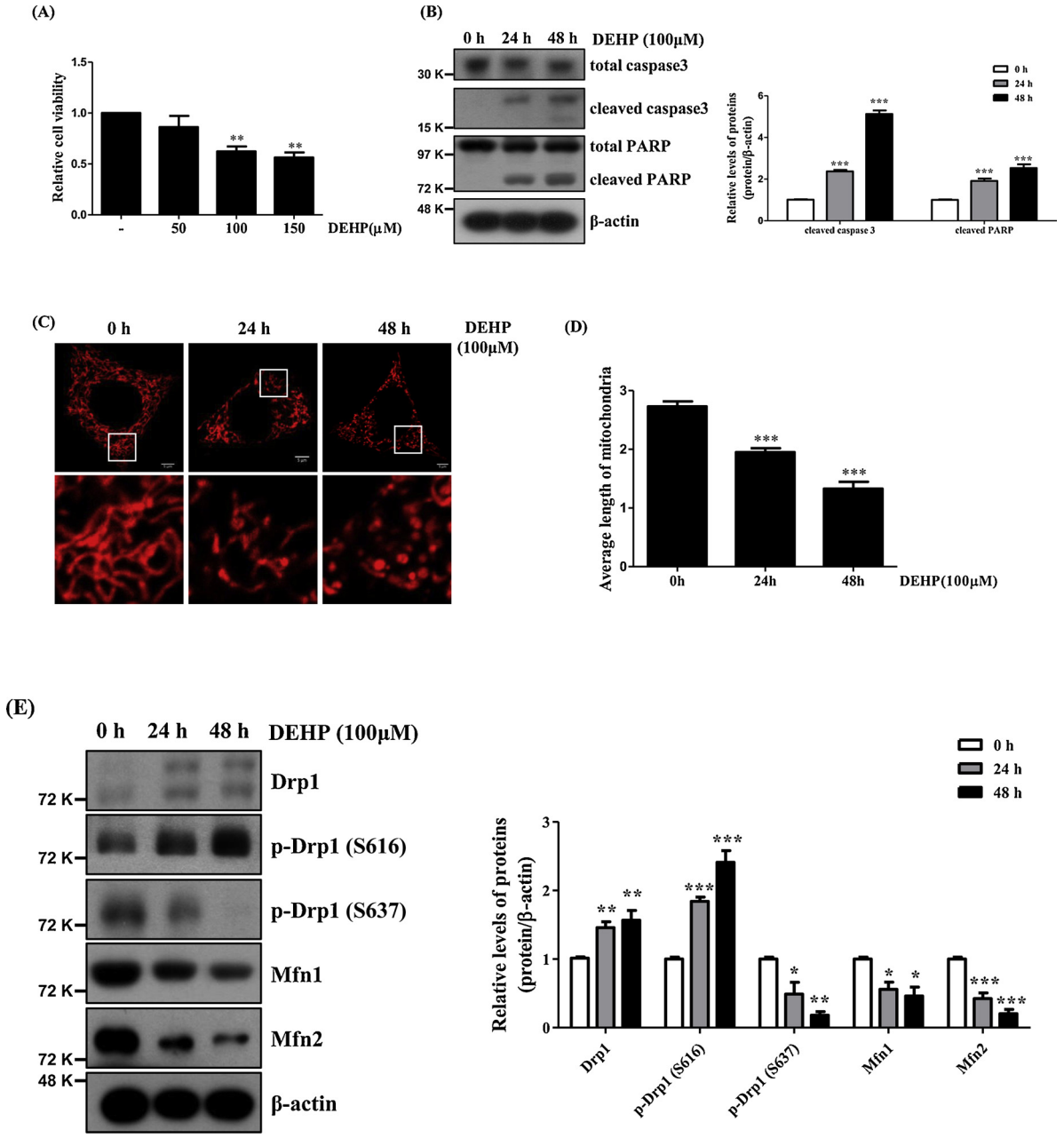

Fig. 1. Determination of mitochondrial fission and neuronal cell death in DEHP-treated HT-22 cells. HT-22 cells were incubated with different concentrations (50–150 μM) of diethylhexyl phthalate (DEHP) for 24 h. (A) Cell viability was confirmed using via CCK assay. (B) The levels of cleaved caspase 3 and cleaved PARP were evaluated via western blotting in DEHP-treated HT-22 cells. (C) Mitochondrial morphology was monitored via confocal microscopy in DEHP-treated HT-22 DsRed2-Mito cells. (D) The average length of mitochondria was measured using ImageJ software. (E) The levels of Drp1, p-Drp1 (Ser637), p-Drp1 (Ser616), Mfn1, and Mfn2 were evaluated using western blotting in DEHP-treated HT-22 cells. Data are presented as mean ± standard deviation (n = 3). *$p < 0.05$, **$p < 0.01$, and ***$p < 0.001$.

one-way ANOVA to analyze comparisons between the control and DEHP groups (Dunnett's Multiple Comparison Test) and between the DEHP and NAC groups (Bonferroni's Multiple Comparison Test). We used two-way ANOVA to analyze the comparison between the HT-22 and HT-22 Prx5 groups. A *p*-value of < 0.05 was deemed to be statistically significant and is indicated on graphs by an asterisk. A *p*-value of < 0.01 and < 0.001 are indicated by two and three asterisks, respectively.

3. Results

3.1. DEHP promotes neuronal cell death and mitochondrial fission in HT-22 cells

To determine the concentration of DEHP that can induce cell death in HT-22 cells, we first assessed cell viability in HT-22 cells cultured with different concentrations (50–150 μM) of DEHP for 24 h. At concentrations above 100 μM, cell viability was significantly lower in DEHP-treated HT-22 cells (Fig. 1A). Based on this observation, we used 100 μM DEHP in the subsequent experiments. To investigate whether DEHP induces apoptosis, we assessed the expression levels of the known apoptotic markers cleaved caspase 3 and cleaved PARP. Levels of both

markers increased in DEHP-treated HT-22 cells at 24 h and 48 h (Fig. 1B). Then, we examined changes in mitochondrial morphology in DEHP-treated HT-22 cells using confocal microscopy. For this, we stably expressed DsRed2-Mito, targeting mitochondria in HT-22 cells. Mitochondria became shorter, and the average mitochondrial length was reduced by DEHP in a time-dependent manner (Fig. 1C and D). Furthermore, phosphorylation and dephosphorylation of Drp1 at serine 616 (Ser616) and serine 637 (Ser637), respectively, activate Drp1 (Cereghetti et al., 2008; Cho et al., 2013). It is also known that Mfn1 and Mfn2 are involved in mitochondrial fusion (Westermann, 2008). Thus, we confirmed changes in the expression of mitochondrial dynamics factors in DEHP-treated HT-22 cells via western blotting. We found that in HT-22 cells, the levels of Drp1 and activated Drp1 (increased phosphorylation at Ser616 and decreased phosphorylation at Ser637) were increased by DEHP, whereas the levels of Mfn1 and Mfn2 were decreased (Fig. 1E). In addition, we investigated alteration in Drp1 localization post DEHP stimulation. Our results indicated that translocation of Drp1 to the mitochondria increased, whereas the level of cytosolic Drp1 decreased (Supplementary Fig. 2A). These findings indicated that DEHP induces mitochondrial fission and neuronal cell death in HT-22 cells.

3.2. NAC attenuates DEHP-induced ROS and mitochondrial ROS production

As DEHP increases ROS levels and an imbalance in mitochondrial dynamics is associated with mitochondrial ROS (Cho et al., 2015; Suen et al., 2008), we confirmed ROS levels and mitochondrial ROS levels in DEHP-treated HT-22 cells with CM-H2DCFDA and MitoSOX, respectively, followed by flow cytometry. Intracellular ROS and mitochondrial ROS levels were significantly increased by DEHP in a time-dependent manner (Fig. 2A and B). Furthermore, to investigate whether DEHP-induced ROS trigger mitochondrial fission and neuronal cell death in HT-22 cells, we used NAC as a ROS scavenger in DEHP-treated HT-22 cells. We confirmed intracellular ROS and mitochondrial ROS in DEHP-treated HT-22 cells with or without NAC treatment for 24 h. DEHP-induced intracellular ROS and mitochondrial ROS levels were attenuated in DEHP-treated HT-22 cells pretreated with NAC compared to that in cells that were not pretreated (Fig. 2C and D). These results indicated that NAC alleviates DEHP-induced intracellular ROS and mitochondrial ROS production in HT-22 cells.

3.3. DEHP-induced ROS triggers mitochondrial fission and neuronal death

As stated above, DEHP increased ROS production in HT-22 cells. ROS activate apoptotic signaling pathways (Redza-Dutordoir and Averill-Bates, 2016). Thus, we investigated the relationship between apoptosis and DEHP-induced ROS using NAC as a ROS scavenger. We assessed the viability of DEHP-treated HT-22 cells untreated or pretreated with NAC. NAC pretreatment attenuated DEHP-induced neuronal cell death (Fig. 3A). Moreover, the expression levels of cleaved caspase 3 and cleaved PARP were decreased by NAC (Fig. 3B). We then investigated the effect of NAC against DEHP-induced mitochondrial fission. HT-22 DsRed2-Mito cells were incubated with 100 μM DEHP in the presence or absence of 5 mM NAC for 24 h, and mitochondrial morphology was observed using confocal microscopy. Pretreatment with NAC ameliorated the shortening of mitochondrial morphology induced by DEHP and mitigated the decreasing average mitochondrial length induced by DEHP (Fig. 3C and D). We also assessed the expression levels of mitochondrial dynamic factors via western blotting and found that NAC attenuates the increasing levels of Drp1 and phosphorylated Drp1 (Ser616) induced by DEHP as well as the decreasing levels of phosphorylated Drp1 (Ser637), Mfn1, and Mfn2 induced by DEHP (Fig. 3E). We also confirmed that NAC attenuated the DEHP-induced Drp1 translocation to the mitochondria (Supplementary Fig. 2A). This meant that NAC attenuates DEHP-induced mitochondrial fission in HT-22 cells. These observations indicated that DEHP-induced ROS mediate DEHP-induced mitochondrial fission and neuronal cell

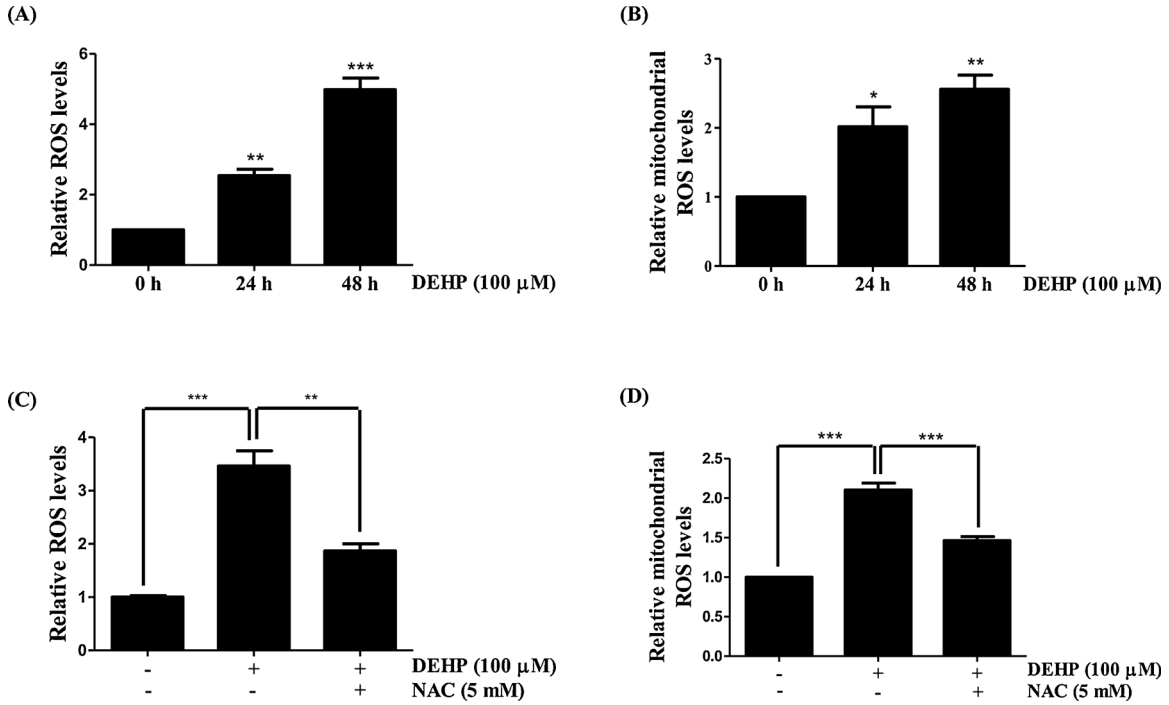

Fig. 2. NAC attenuated DEHP-induced intracellular and mitochondrial ROS production. (A and B) HT-22 cells were incubated with 100 μM DEHP for 24 h and 48 h, and intracellular (A) and mitochondrial ROS (B) levels were measured using CM-H_2DCFDA and Mito-SOX, respectively, via flow cytometry. (C and D) HT-22 cells were cultured with or without 5 mM NAC for 30 min before treatment with 100 μM DEHP for 24 h, and intracellular (C) and mitochondrial ROS (D) levels were measured using CM-H_2DCFDA and Mito-SOX, respectively, via flow cytometry. Data are presented as mean ± standard deviation (n = 3). *$p < 0.05$, **$p < 0.01$, and ***$p < 0.001$.

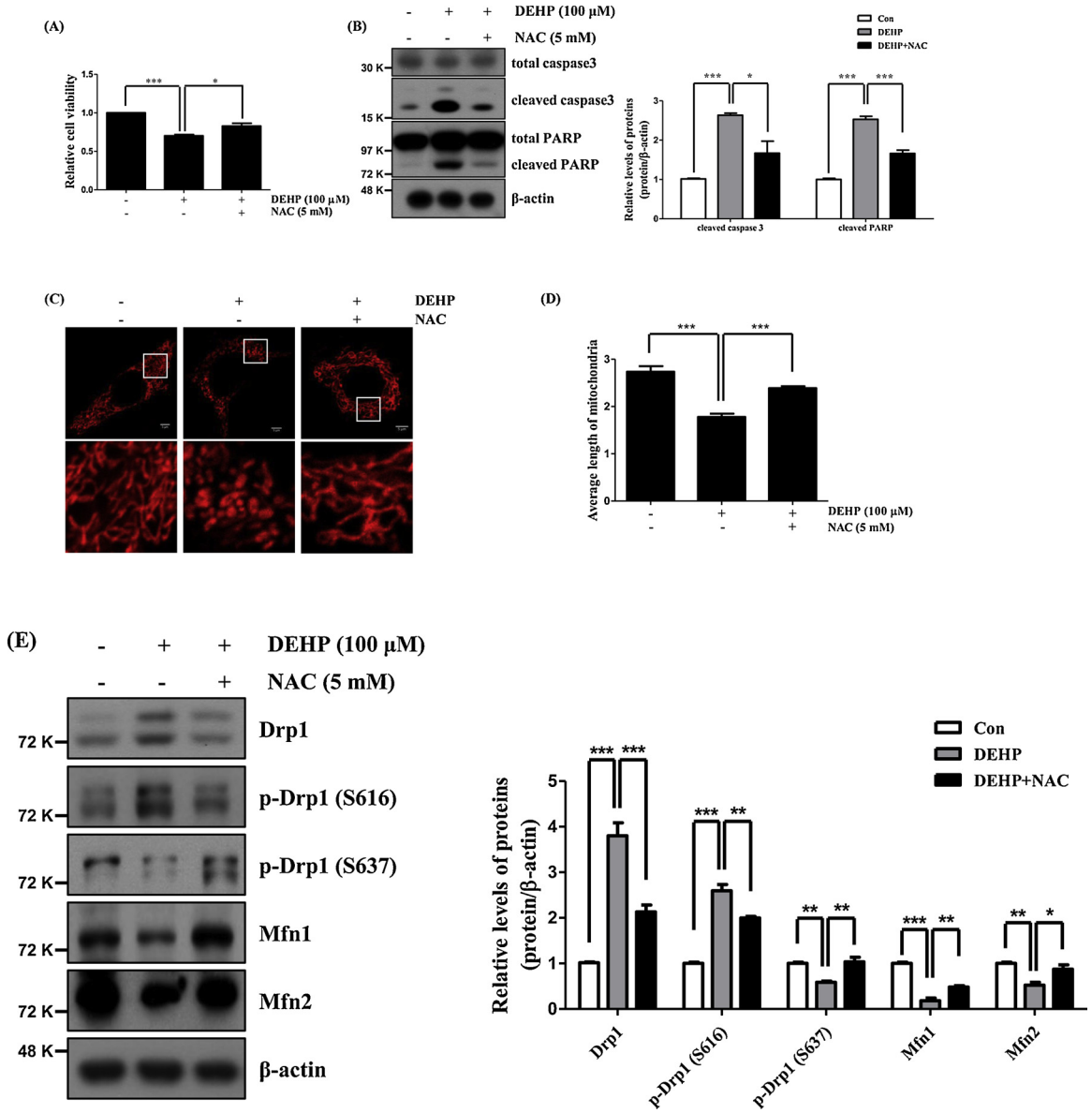

Fig. 3. NAC attenuated DEHP-induced mitochondrial fission and neuronal cell death. HT-22 cells were incubated with or without 5 mM NAC for 30 min before treatment with 100 μM DEHP for 24 h. (A) Cell viability was assessed via CCK assay. (B) The levels of cleaved caspase 3 and cleaved PARP were confirmed using western blotting. (C) Mitochondrial morphology was observed using confocal microscopy in DEHP-treated HT-22 DsRed2-mito cells with or without NAC. (D) The average length of mitochondria was measured using ImageJ software. (E) The levels of Drp1, p-Drp1 (Ser637), p-Drp1 (Ser616), Mfn1, and Mfn2 were evaluated using western blotting. Data are presented as mean ± standard deviation (n = 3). *p < 0.05, **p < 0.01, and ***p < 0.001.

death in HT-22 cells.

3.4. Prx5 attenuates DEHP-induced ROS production

Previous studies have shown that Prx5 exhibits protective effects against neurotoxicity (Kim et al., 2016; Lee et al., 2018). As shown in Fig. 3, we found that DEHP-induced ROS play an important role in DEHP-induced mitochondrial fission and neuronal death in HT-22 cells. Therefore, we hypothesized that Prxs might be protective against DEHP-induced neurotoxicity. Thus, we first checked the expression levels of Prxs in DEHP-treated HT-22 cells using western blotting and observed that Prx5 levels were significantly increased by DEHP, whereas Prx1, Prx2, Prx3, Prx4, and Prx6 levels hardly changed in DEHP-treated HT-22 cells (Fig. 4A). These observations suggested that Prx5 has a protective effect against DEHP-induced neurotoxicity. To investigate the role of Prx5 in DEHP-induced neurotoxicity, we generated constitutively Prx5-expressing HT-22 cells using a V5-tagged Prx5 (Prx5-V5) lentiviral vector. We verified the expression of Prx5-V5 by western blotting with V5 antibody (Fig. 4B). Then, we confirmed whether Prx5 overexpression effectively reduces the levels of intracellular ROS and mitochondrial ROS in DEHP-treated HT-22 cells using flow cytometry. We found that overexpression of Prx5 lowers DEHP-induced intracellular and mitochondrial ROS production (Fig. 4C and D). These results suggested that Prx5 protects against DEHP-induced neurotoxicity by inhibiting ROS production in HT-22 cells.

3.5. Prx5 attenuates DEHP-induced mitochondrial fission and neuronal cell death

The protective effect of Prx5 against DEHP-induced neuronal cell death was examined by CCK assay and western blotting in HT-22 and HT-22 Prx5 cells. Prx5 overexpression decreased neuronal cell death induced by DEHP in DEHP-treated HT-22 cells (Fig. 5A) as well as the levels of cleaved caspase 3 and cleaved PARP (Fig. 5B). These findings

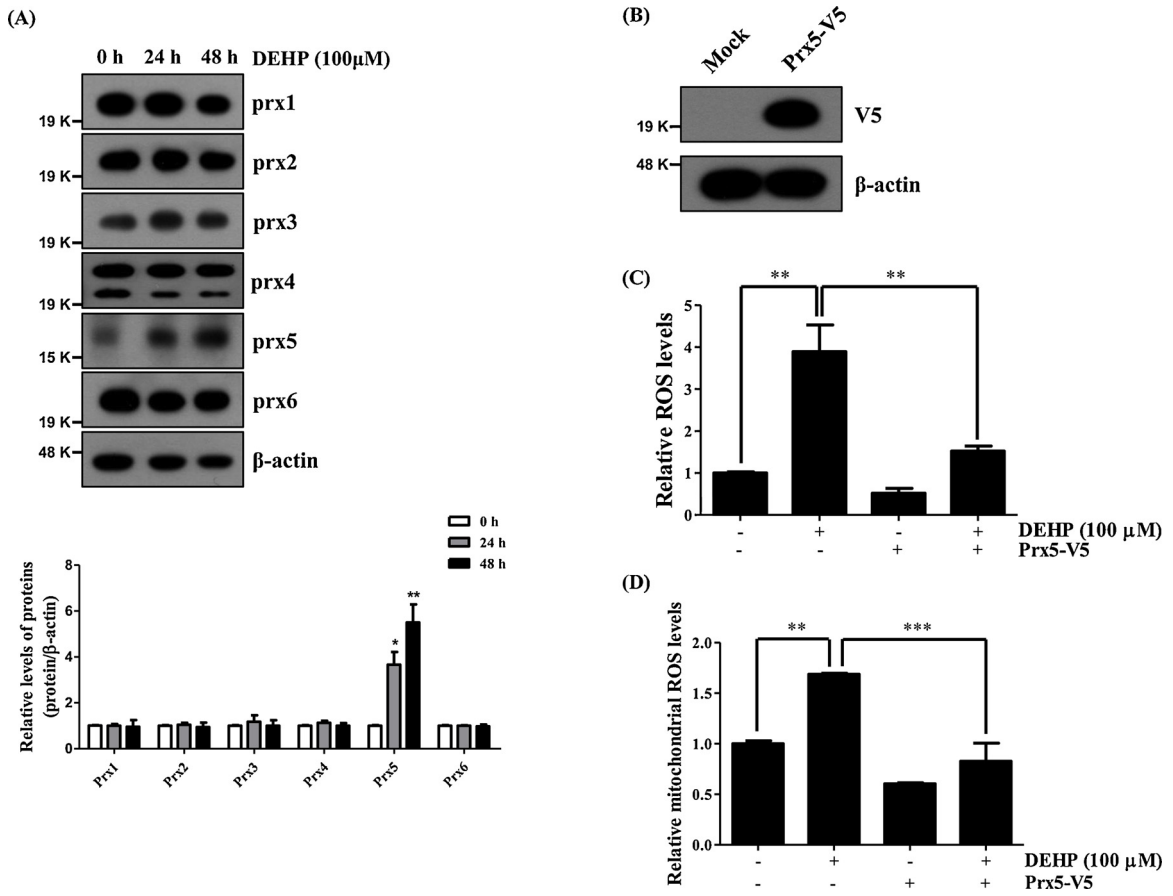

Fig. 4. Prx5 attenuated DEHP-induced ROS production. HT-22 cells were cultured with 100 μM DEHP for 24 h and 48 h. (A) The levels of Prx1, Prx2, Prx3, Prx4, Prx5, and Prx6 were confirmed by western blotting. (B) Constitutively Prx5-expressing HT-22 cells were verified using western blotting with anti-V5 antibody. (C and D) HT-22 and HT-22 Prx5 cells were incubated with or without DEHP for 24 h, and intracellular (C) and mitochondrial (D) ROS levels were measured with CM-H_2DCFDA and Mito-SOX, respectively, via flow cytometry. Data are presented as mean ± standard deviation (n = 3). *p < 0.05, **p < 0.01, and ***p < 0.001.

indicated that Prx5 ameliorates DEHP-induced neuronal cell death by reducing ROS. We studied whether Prx5 overexpression affects DEHP-induced mitochondrial fission using confocal microscopy and western blotting and observed that Prx5 overexpression alleviates the mitochondrial morphology changes and mitochondrial shortening induced by DEHP in DEHP-treated HT-22 cells (Fig. 5C and D). Prx5 overexpression also decreased the levels of Drp1 and phosphorylated Drp1 (Ser616) and increased the levels of phosphorylated Drp1 (Ser637), Mfn1, and Mfn2 in DEHP-treated HT-22 cells (Fig. 5E). Moreover, Prx5 also alleviated Drp1 translocation to the mitochondria compared to that in DEHP-treated HT-22 cells (Supplementary Fig. 2B). These findings indicated that Prx5 has protective effects against DEHP-induced neurotoxicity by inhibiting ROS-mediated mitochondrial fission in HT-22 cells.

3.6. Knockdown of Prx5 exacerbates DEHP-induced mitochondrial fission and neuronal cell death

To further investigate the role of Prx5 against DEHP-induced neurotoxicity, we used Prx5-silenced HT-22 cells using siPrx5 transfection. We identified knockdown of endogenous Prx5 by western blotting in siPrx5-transfected HT-22 cells with or without DEHP (Fig. 6A). Subsequently, we investigated the effect of Prx5 knockdown against DEHP-induced neuronal cell death and ROS production. The results showed that Prx5 silencing exacerbates DEHP-induced ROS production and neuronal cell death (Fig. 6B and C). Prx5 silencing also increased the levels of cleaved caspase3 and cleaved PARP compared to that in DEHP-treated HT-22 cells (Fig. 6D). Moreover, we investigated the effect of siPrx5 against DEHP-induced mitochondrial fission using confocal microscopy and western blotting. Our results showed that siPrx5 aggravates DEHP-induced mitochondrial morphology changes and mitochondrial shortening (Fig. 6E). Also, siPrx5 increased the levels of Drp1 and phosphorylated Drp1 (Ser616) and decreased the levels of phosphorylated Drp1 (Ser637), Mfn1, and Mfn2 in DEHP-treated HT-22 cells (Fig. 6F). In addition, siPrx5 increased Drp1 translocation to the mitochondria much more compared to that in DEHP-treated HT-22 cells (Supplementary Fig. 2B). These results indicated that knockdown of endogenous Prx5 worsens DEHP-induced mitochondrial fission and neuronal cell death.

4. Discussion

Phthalates are used as plasticizers; however, they are not covalently bound to products, and therefore, humans are easily exposed to them (Holahan and Smith, 2015). DEHP, the most common phthalate, affects neurons—especially in the hippocampus (Barakat et al., 2018)—as well as reproduction, development, and the endocrine system (Chen et al., 2015; Erkekoglu et al., 2011; Tyl et al., 1988). Several studies have identified that DEHP induces apoptosis by mediating endoplasmic reticulum stress, autophagy, and mitochondrial dysfunction (Fu et al., 2017; Sun et al., 2015, 2018). Imbalances of mitochondrial dynamics induce mitochondrial dysfunction and apoptosis (Chen et al., 2005; Suen et al., 2008; Westermann, 2012). However, the link between DEHP and mitochondrial dynamics has not been well studied, and a detailed understanding is lacking. We, therefore, investigated the relationship between neuronal cell death and mitochondrial dynamics

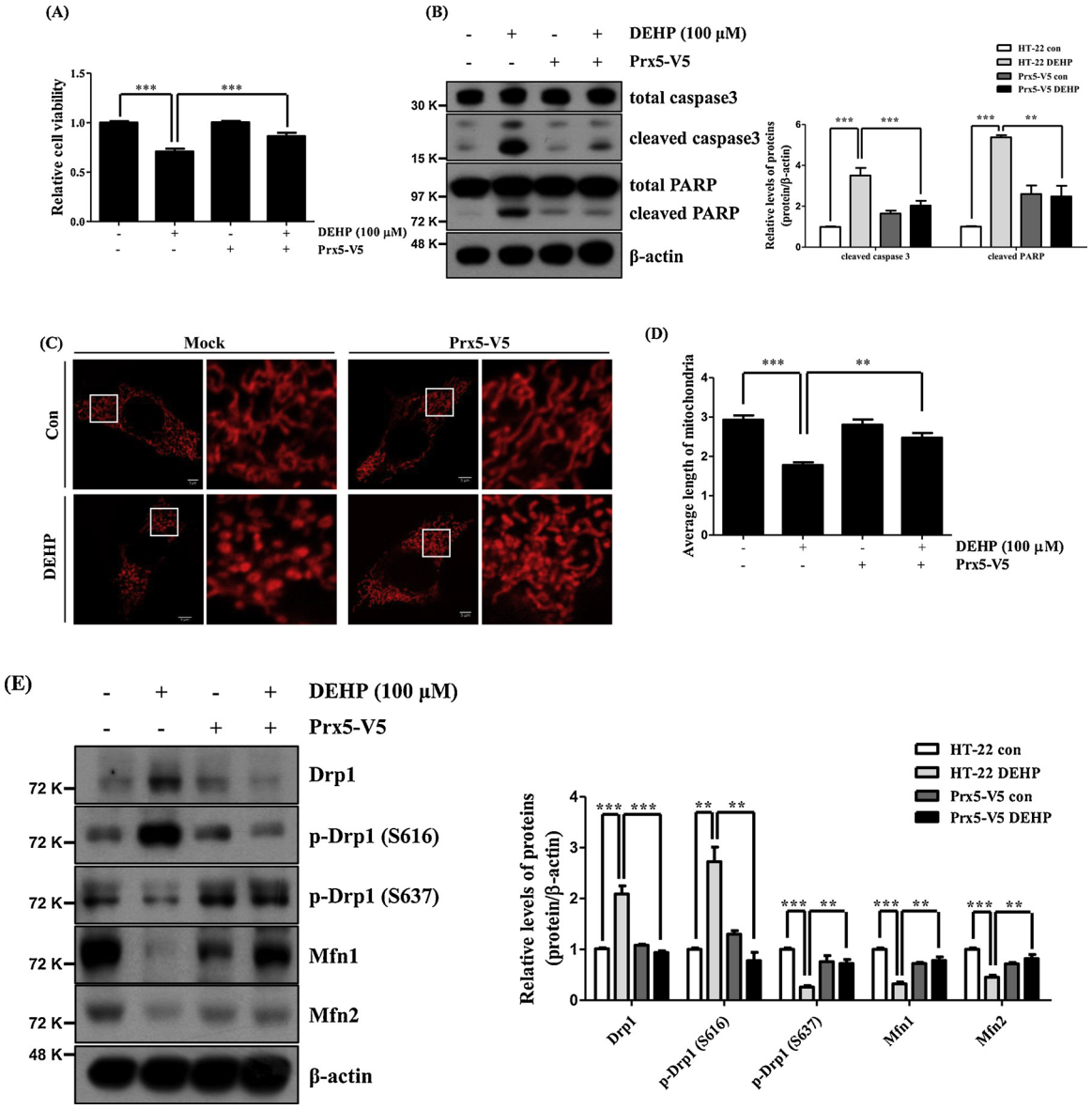

Fig. 5. Prx5 ameliorated DEHP-induced mitochondrial fission and neuronal cell death. HT-22 and HT-22 Prx5 cells were incubated with or without 100 μM DEHP for 24 h. (A) Cell viability was measured via CCK assay. (B) The levels of cleaved caspase 3 and cleaved PARP were confirmed using western blotting. (C) Mitochondrial morphology was observed using confocal microscopy in *DsRed2-Mito*-transfected HT-22 and HT-22 Prx5 cells with or without DEHP. (D) The average mitochondria length was measured using ImageJ software. (E) The levels of Drp1, p-Drp1 (Ser637), p-Drp1 (Ser616), Mfn1, and Mfn2 were confirmed via western blotting. Data are presented as mean ± standard deviation (n = 3). **p < 0.01 and ***p < 0.001.

mediated by DEHP in mouse hippocampal neuron-derived HT-22 cells.

We first identified the effect of DEHP on neuronal cell death and mitochondrial dynamics in HT-22 cells. As mentioned previously, mitochondrial fusion is regulated by Mfn1/2, and mitochondrial fission is regulated by Drp1, which is activated by its phosphorylation status, at Ser616 (phosphorylation) and Ser637 (dephosphorylation) (Cho et al., 2010; Knott et al., 2008). As shown in Fig. 1, DEHP induced neuronal cell death as well as mitochondrial fission via Drp1 activation (phosphorylation and dephosphorylation of Ser616 and Ser637, respectively) and decreased levels of Mfn1 and Mfn2. Oxidative stress plays a role in mitochondrial dysfunction and caspase activation, and both induce apoptosis (Hung et al., 2018; Ott et al., 2007). Previous research has reported ROS induction by DEHP in primary cortical cells (Wojtowicz et al., 2019). Furthermore, there is a strong correlation between mitochondrial fission and mitochondrial ROS (Wu et al., 2011). Therefore, we thought that ROS might play a crucial role in DEHP-induced mitochondrial fission and neuronal cell death. Thus, we investigated whether DEHP-induced mitochondrial fission and neuronal cell death were mediated by ROS. As shown in Fig. 2, the levels of intracellular ROS and mitochondrial ROS were increased by DEHP in a time-dependent manner, and pretreatment with NAC, a ROS scavenger, attenuated DEHP-induced ROS production. NAC also ameliorated DEHP-induced mitochondrial fission and neuronal cell death (Fig. 3). We further investigated the relationship between DEHP-induced mitochondrial fission and neuronal cell death. We used Mdivi-1 as an inhibitor of mitochondrial fission because many studies have reported that Mdivi-1, a cell-permeable quinazolinone, acts as an inhibitor of Drp1 and inhibits excessive mitochondrial fission (Cassidy-Stone et al., 2008; Manczak et al., 2019; Smith and Gallo, 2017). Inhibition of mitochondrial fission and mitochondrial ROS production, using Mdivi-1 and mito-TEMPO respectively, mitigated DEHP-induced mitochondrial fission and neuronal cell death (Supplementary Fig. 1). Moreover, to clearly elucidate the relationship between DEHP-induced mitochondrial fission and neuronal cell death, we compared the time course of both

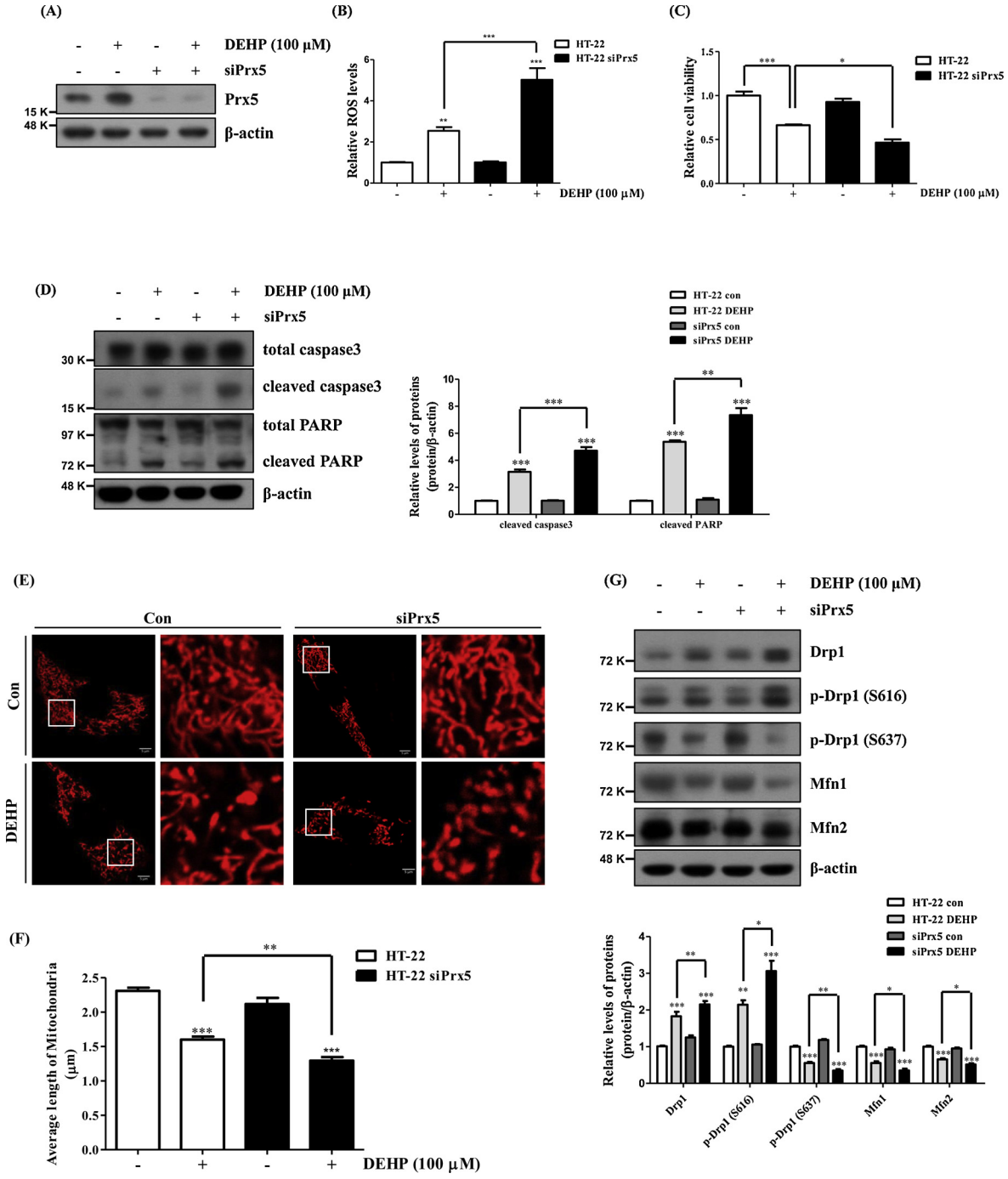

Fig. 6. Knockdown of Prx5 aggravated DEHP-induced mitochondrial fission and neuronal cell death. HT-22 and HT-22 siPrx5 cells were incubated with or without 100 μM DEHP for 24 h. (A) The levels of Prx5 were assessed using western blotting. (B) Intracellular ROS levels were measured with CM-H_2DCFDA via flow cytometry. (C) Cell viability was measured via CCK assay. (D) The levels of cleaved caspase 3 and cleaved PARP were confirmed using western blotting. (E) Mitochondrial morphology was observed using confocal microscopy in *DsRed2-Mito*-transfected HT-22 and HT-22 siPrx5 cells with or without DEHP. (F) The average mitochondrial length was measured using ImageJ software. (G) The levels of Drp1, p-Drp1 (Ser637), p-Drp1 (Ser616), Mfn1, and Mfn2 were confirmed via western blotting. Data are presented as mean ± standard deviation (n = 3). **p < 0.01 and ***p < 0.001.

mitochondrial fission and apoptosis. DEHP caused apoptosis after 24 h, whereas factors associated with mitochondrial dynamics altered after 9 h (Supplementary Fig. 3A and B). The usage of Mdivi-1 to inhibit mitochondrial fission is a bit controversial in research circles (Bordt et al., 2017; Smith and Gallo, 2017); therefore, we provide additional evidence of mitochondrial fission-mediated neuronal death by DEHP stimulation. We used mutant Drp1 (K38A) stably expressing HT-22 cells. This GTPase-deficient mutation in Drp1 converts lysine into alanine in the consensus G1 motif of the GTPase domain, thereby inhibiting GTP binding by Drp1 (Ugarte-Uribe et al., 2014). Our results showed that dominant-negative mutation in Drp1 alleviates DEHP-induced neuronal cell death and mitochondrial fission (Supplementary Fig. 3C–F). These results indicated that DEHP-induced ROS causes mitochondrial fission, and consequently triggers neuronal cell death in HT-22 cells.

The glutathione system protects the brain from oxidative stress (Dringen and Hirrlinger, 2003). However, there is increasing evidence that Prxs are also important antioxidants and play a protective role in

neurological damage, such as oxidative and inflammatory stresses (Bell and Hardingham, 2011; Zhu et al., 2012). Furthermore, previous studies have identified that Prx5 protects neuronal cells against neurological damage, including oxidative stress, inflammation and mitochondrial damage (Kim et al., 2016; Lee et al., 2018; Park et al., 2016). Because DEHP induced ROS production (Fig. 2A and B), we investigated the expression levels of Prxs in DEHP-treated HT-22 cells to study the relationship between DEHP-induced neurotoxicity and Prxs. We found that among the Prxs, only Prx5 was significantly increased by DEHP (Fig. 4A). Therefore, we hypothesized that Prx5 might have a protective effect against DEHP-induced neurotoxicity in HT-22 cells. Thus, we investigated the effects of Prx5 in DEHP-induced mitochondrial fission and neuronal cell death by overexpressing or silencing Prx5 in HT-22 cells. As shown in Figs. 4B and 6A, we confirmed the overexpression of Prx5-V5 and the silencing of endogenous Prx5 using anti-V5 and anti-Prx5 antibodies, respectively. We also found that Prx5 overexpression attenuates DEHP-induced ROS production, whereas Prx5 knockdown aggravates it (Figs. 4C, D and 6B). Furthermore, Prx5 overexpression ameliorated DEHP-induced mitochondrial fission and neuronal cell death (Fig. 5), whereas Prx5 silencing led to its aggravation (Fig. 6). Several studies have shown that mitochondrial dynamics are closely associated with mitochondrial functions, including mitochondrial respiration (Galloway et al., 2012; Zorzano et al., 2010). Thus, we investigated the effects of Prx5 against DEHP-induced alteration of oxygen consumption rate (OCR). As shown in Supplementary Fig. 4, Prx5 alleviated ROS-dependent OCR reduction induced by DEHP, whereas siPrx5 exacerbated it. These findings indicated that Prx5 has a protective effect against DEHP-induced mitochondrial dysfunction (excessive fission and impairment of respiration) and neuronal cell death, by inhibiting ROS production.

In conclusion, we demonstrated, for the first time, that DEHP-induced mitochondrial fission and neuronal cell death are ROS-dependent. Moreover, we found that Prx5, which is induced by DEHP, has a protective effect against DEHP-induced neuronal cell death and mitochondrial dysfunction by reducing ROS production. Our findings suggested that Prx5 plays important roles in DEHP-induced neurotoxicity, and our results may provide a new therapeutic target for diseases related to DEHP neurotoxicity.

Declaration of Competing Interest

The authors declare no conflict of interest.

Acknowledgments

This research was supported by grants from the KRIBB Research Initiative Program (KGM4621922) and the National Research Foundation of Korea, funded by the Republic of Korea government (NRF-2015R1A4A1042271, NRF-2017R1A2B4008176, and NRF-2017R1A5A2015391).

Appendix A. Supplementary data

Supplementary material related to this article can be found, in the online version, at doi:https://doi.org/10.1016/j.neuro.2019.08.003.

References

Barakat, R., Lin, P.C., Park, C.J., Best-Popescu, C., Bakry, H.H., Abosalem, M.E., Abdelaleem, N.M., Flaws, J.A., Ko, C., 2018. Prenatal exposure to DEHP induces neuronal degeneration and neurobehavioral abnormalities in adult male mice. Toxicol. Sci. 164 (2), 439–452.

Bell, K.F., Hardingham, G.E., 2011. CNS peroxiredoxins and their regulation in health and disease. Antioxid. Redox Signal. 14 (8), 1467–1477.

Berlett, B.S., Stadtman, E.R., 1997. Protein oxidation in aging, disease, and oxidative stress. J. Biol. Chem. 272 (33), 20313–20316.

Bordt, E.A., Clerc, P., Roelofs, B.A., Saladino, A.J., Tretter, L., Adam-Vizi, V., Cherok, E., Khalil, A., Yadava, N., Ge, S.X., Francis, T.C., Kennedy, N.W., Picton, L.K., Kumar, T., Uppuluri, S., Miller, A.M., Itoh, K., Karbowski, M., Sesaki, H., Hill, R.B., Polster, B.M., 2017. The putative Drp1 inhibitor mdivi-1 is a reversible mitochondrial complex I inhibitor that modulates reactive oxygen species. Dev. Cell 40 (6), 583–594 e586.

Cassidy-Stone, A., Chipuk, J.E., Ingerman, E., Song, C., Yoo, C., Kuwana, T., Kurth, M.J., Shaw, J.T., Hinshaw, J.E., Green, D.R., Nunnari, J., 2008. Chemical inhibition of the mitochondrial division dynamin reveals its role in Bax/Bak-dependent mitochondrial outer membrane permeabilization. Dev. Cell 14 (2), 193–204.

Cereghetti, G.M., Stangherlin, A., Martins de Brito, O., Chang, C.R., Blackstone, C., Bernardi, P., Scorrano, L., 2008. Dephosphorylation by calcineurin regulates translocation of Drp1 to mitochondria. Proc. Natl. Acad. Sci. U. S. A. 105 (41), 15803–15808.

Chen, H., Chomyn, A., Chan, D.C., 2005. Disruption of fusion results in mitochondrial heterogeneity and dysfunction. J. Biol. Chem. 280 (28), 26185–26192.

Chen, J., Wu, S., Wen, S., Shen, L., Peng, J., Yan, C., Cao, X., Zhou, Y., Long, C., Lin, T., He, D., Hua, Y., Wei, G., 2015. The mechanism of environmental endocrine disruptors (DEHP) induces epigenetic transgenerational inheritance of cryptorchidism. PLoS One 10 (6), e0126403.

Cho, B., Choi, S.Y., Cho, H.M., Kim, H.J., Sun, W., 2013. Physiological and pathological significance of dynamin-related protein 1 (drp1)-dependent mitochondrial fission in the nervous system. Exp. Neurobiol. 22 (3), 149–157.

Cho, D.H., Nakamura, T., Lipton, S.A., 2010. Mitochondrial dynamics in cell death and neurodegeneration. Cell. Mol. Life Sci. 67 (20), 3435–3447.

Cho, Y.J., Park, S.B., Han, M., 2015. Di-(2-ethylhexyl)-phthalate induces oxidative stress in human endometrial stromal cells in vitro. Mol. Cell. Endocrinol. 407, 9–17.

Coluzzi, E., Colamartino, M., Cozzi, R., Leone, S., Meneghini, C., O'Callaghan, N., Sgura, A., 2014. Oxidative stress induces persistent telomeric DNA damage responsible for nuclear morphology change in mammalian cells. PLoS One 9 (10), e110963.

Davis, J.B., Maher, P., 1994. Protein kinase C activation inhibits glutamate-induced cytotoxicity in a neuronal cell line. Brain Res. 652 (1), 169–173.

Dringen, R., Hirrlinger, J., 2003. Glutathione pathways in the brain. Biol. Chem. 384 (4), 505–516.

Erkekoglu, P., Zeybek, N.D., Giray, B., Asan, E., Arnaud, J., Hincal, F., 2011. Reproductive toxicity of di(2-ethylhexyl) phthalate in selenium-supplemented and selenium-deficient rats. Drug Chem. Toxicol. 34 (4), 379–389.

Fu, G., Dai, J., Zhang, D., Zhu, L., Tang, X., Zhang, L., Zhou, T., Duan, P., Quan, C., Zhang, Z., Song, S., Shi, Y., 2017. Di(2-ethylhexyl) phthalate induces apoptosis through mitochondrial pathway in GC-2spd cells. Environ. Toxicol. 32 (3), 1055–1064.

Galloway, C.A., Lee, H., Yoon, Y., 2012. Mitochondrial morphology-emerging role in bioenergetics. Free Radic. Biol. Med. 53 (12), 2218–2228.

Hampton, M.B., O'Connor, K.M., 2016. Peroxiredoxins and the regulation of cell death. Mol. Cells 39 (1), 72–76.

Hauck, A.K., Bernlohr, D.A., 2016. Oxidative stress and lipotoxicity. J. Lipid Res. 57 (11), 1976–1986.

Holahan, M.R., Smith, C.A., 2015. Phthalates and neurotoxic effects on hippocampal network plasticity. Neurotoxicology 48, 21–34.

Hung, C.H., Cheng, S.S., Cheung, Y.T., Wuwongse, S., Zhang, N.Q., Ho, Y.S., Lee, S.M., Chang, R.C., 2018. A reciprocal relationship between reactive oxygen species and mitochondrial dynamics in neurodegeneration. Redox Biol. 14, 7–19.

Kang, S.W., Rhee, S.G., Chang, T.S., Jeong, W., Choi, M.H., 2005. 2-Cys peroxiredoxin function in intracellular signal transduction: therapeutic implications. Trends Mol. Med. 11 (12), 571–578.

Kim, B., Park, J., Chang, K.T., Lee, D.S., 2016. Peroxiredoxin 5 prevents amyloid-beta oligomer-induced neuronal cell death by inhibiting ERK-Drp1-mediated mitochondrial fragmentation. Free Radic. Biol. Med. 90, 184–194.

Knoops, B., Goemaere, J., Van der Eecken, V., Declercq, J.P., 2011. Peroxiredoxin 5: structure, mechanism, and function of the mammalian atypical 2-Cys peroxiredoxin. Antioxid. Redox Signal. 15 (3), 817–829.

Knott, A.B., Perkins, G., Schwarzenbacher, R., Bossy-Wetzel, E., 2008. Mitochondrial fragmentation in neurodegeneration. Nat. Rev. Neurosci. 9 (7), 505–518.

Lee, D.G., Kam, M.K., Kim, K.M., Kim, H.S., Kwon, O.S., Lee, H.S., Lee, D.S., 2018. Peroxiredoxin 5 prevents iron overload-induced neuronal death by inhibiting mitochondrial fragmentation and endoplasmic reticulum stress in mouse hippocampal HT-22 cells. Int. J. Biochem. Cell Biol. 102, 10–19.

Lee, J., Lee, J.H., Kim, C.K., Thomsen, M., 2014. Childhood exposure to DEHP, DBP and BBP under existing chemical management systems: a comparative study of sources of childhood exposure in Korea and in Denmark. Environ. Int. 63, 77–91.

Manczak, M., Kandimalla, R., Yin, X., Reddy, P.H., 2019. Mitochondrial division inhibitor 1 reduces dynamin-related protein 1 and mitochondrial fission activity. Hum. Mol. Genet. 28 (2), 177–199.

McCarron, J.G., Wilson, C., Sandison, M.E., Olson, M.L., Girkin, J.M., Saunter, C., Chalmers, S., 2013. From structure to function: mitochondrial morphology, motion and shaping in vascular smooth muscle. J. Vasc. Res. 50 (5), 357–371.

Otera, H., Mihara, K., 2012. Mitochondrial dynamics: functional link with apoptosis. Int. J. Cell Biol. 2012, 821676.

Ott, M., Gogvadze, V., Orrenius, S., Zhivotovsky, B., 2007. Mitochondria, oxidative stress and cell death. Apoptosis 12 (5), 913–922.

Park, J., Choi, H., Kim, B., Chae, U., Lee, D.G., Lee, S.R., Lee, S., Lee, H.S., Lee, D.S., 2016. Peroxiredoxin 5 (Prx5) decreases LPS-induced microglial activation through regulation of Ca(2+)/calcineurin-Drp1-dependent mitochondrial fission. Free Radic. Biol. Med. 99, 392–404.

Park, J., Choi, H., Min, J.S., Kim, B., Lee, S.R., Yun, J.W., Choi, M.S., Chang, K.T., Lee, D.S., 2015. Loss of mitofusin 2 links beta-amyloid-mediated mitochondrial fragmentation and Cdk5-induced oxidative stress in neuron cells. J. Neurochem. 132 (6), 687–702.

Picard, M., Shirihai, O.S., Gentil, B.J., Burelle, Y., 2013. Mitochondrial morphology transitions and functions: implications for retrograde signaling? Am. J. Physiol.

Regul. Integr. Comp. Physiol. 304 (6), R393–406.
Redza-Dutordoir, M., Averill-Bates, D.A., 2016. Activation of apoptosis signalling pathways by reactive oxygen species. Biochim. Biophys. Acta 1863 (12), 2977–2992.
Rhee, S.G., Yang, K.S., Kang, S.W., Woo, H.A., Chang, T.S., 2005. Controlled elimination of intracellular H(2)O(2): regulation of peroxiredoxin, catalase, and glutathione peroxidase via post-translational modification. Antioxid. Redox Signal. 7 (5–6), 619–626.
Rowdhwal, S.S.S., Chen, J., 2018. Toxic effects of Di-2-ethylhexyl phthalate: an overview. Biomed Res. Int. 2018, 1750368.
Ryter, S.W., Kim, H.P., Hoetzel, A., Park, J.W., Nakahira, K., Wang, X., Choi, A.M., 2007. Mechanisms of cell death in oxidative stress. Antioxid. Redox Signal. 9 (1), 49–89.
Smith, G., Gallo, G., 2017. To mdivi-1 or not to mdivi-1: Is that the question? Dev. Neurobiol. 77 (11), 1260–1268.
Suen, D.F., Norris, K.L., Youle, R.J., 2008. Mitochondrial dynamics and apoptosis. Genes Dev. 22 (12), 1577–1590.
Sun, X., Lin, Y., Huang, Q., Shi, J., Qiu, L., Kang, M., Chen, Y., Fang, C., Ye, T., Dong, S., 2015. Di(2-ethylhexyl) phthalate-induced apoptosis in rat INS-1 cells is dependent on activation of endoplasmic reticulum stress and suppression of antioxidant protection. J. Cell. Mol. Med. 19 (3), 581–594.
Sun, Y., Shen, J., Zeng, L., Yang, D., Shao, S., Wang, J., Wei, J., Xiong, J., Chen, J., 2018. Role of autophagy in di-2-ethylhexyl phthalate (DEHP)-induced apoptosis in mouse Leydig cells. Environ. Pollut. 243 (Pt A), 563–572.
Tyl, R.W., Price, C.J., Marr, M.C., Kimmel, C.A., 1988. Developmental toxicity evaluation of dietary di(2-ethylhexyl)phthalate in Fischer 344 rats and CD-1 mice. Fundam. Appl. Toxicol. 10 (3), 395–412.
Ugarte-Uribe, B., Muller, H.M., Otsuki, M., Nickel, W., Garcia-Saez, A.J., 2014. Dynamin-related protein 1 (Drp1) promotes structural intermediates of membrane division. J. Biol. Chem. 289 (44), 30645–30656.
Westermann, B., 2008. Molecular machinery of mitochondrial fusion and fission. J. Biol. Chem. 283 (20), 13501–13505.
Westermann, B., 2012. Bioenergetic role of mitochondrial fusion and fission. Biochim. Biophys. Acta 1817 (10), 1833–1838.
Wojtowicz, A.K., Sitarz-Glownia, A.M., Szczesna, M., Szychowski, K.A., 2019. The action of di-(2-Ethylhexyl) phthalate (DEHP) in mouse cerebral cells involves an impairment in aryl hydrocarbon receptor (AhR) signaling. Neurotox. Res. 35 (1), 183–195.
Wu, S., Zhou, F., Zhang, Z., Xing, D., 2011. Mitochondrial oxidative stress causes mitochondrial fragmentation via differential modulation of mitochondrial fission-fusion proteins. FEBS J. 278 (6), 941–954.
Zhang, C., Xie, M., Chen, J., Zhang, Y., Wei, S., Ma, X., Xiao, L., Chen, L., 2018. UV-B radiation induces DEHP degradation and their combined toxicological effects on Scenedesmus acuminatus. Aquat. Toxicol. 203, 172–178.
Zhu, H., Santo, A., Li, Y., 2012. The antioxidant enzyme peroxiredoxin and its protective role in neurological disorders. Exp. Biol. Med. (Maywood) 237 (2), 143–149.
Zorzano, A., Liesa, M., Sebastian, D., Segales, J., Palacin, M., 2010. Mitochondrial fusion proteins: dual regulators of morphology and metabolism. Semin. Cell Dev. Biol. 21 (6), 566–574.